Received: 23 January 2024 | Revised: 24 March 2024 | Accepted: 25 March 2024

DOI: 10.1111/mmi.15262

RESEARCH ARTICLE

WILEY

Intermembrane space-localized TbTim15 is an essential subunit of the single mitochondrial inner membrane protein translocase of trypanosomes

Corinne von Känel[1] | Silke Oeljeklaus[2] | Christoph Wenger[1] | Philip Stettler[1] | Anke Harsman[1] | Bettina Warscheid[2] | André Schneider[1]

[1]Department of Chemistry, Biochemistry and Pharmaceutical Sciences, University of Bern, Bern, Switzerland

[2]Faculty of Chemistry and Pharmacy, Biochemistry II, Theodor Boveri-Institute, University of Würzburg, Würzburg, Germany

Correspondence
André Schneider, Department of Chemistry, Biochemistry and Pharmaceutical Sciences, University of Bern, Freiestrasse 3, Bern, Switzerland.
Email: andre.schneider@unibe.ch

Funding information
NCCR RNA & Disease; National Centre of Competence in Research, Grant/Award Number: 205601; Swiss National Science Foundation, Grant/Award Number: SNF 205200

Abstract

All mitochondria import >95% of their proteins from the cytosol. This process is mediated by protein translocases in the mitochondrial membranes, whose subunits are generally highly conserved. Most eukaryotes have two inner membrane protein translocases (TIMs) that are specialized to import either presequence-containing or mitochondrial carrier proteins. In contrast, the parasitic protozoan *Trypanosoma brucei* has a single TIM complex consisting of one conserved and five unique subunits. Here, we identify candidates for new subunits of the TIM or the presequence translocase-associated motor (PAM) using a protein–protein interaction network of previously characterized TIM and PAM subunits. This analysis reveals that the trypanosomal TIM complex contains an additional trypanosomatid-specific subunit, designated TbTim15. TbTim15 is associated with the TIM complex, lacks transmembrane domains, and localizes to the intermembrane space. TbTim15 is essential for procyclic and bloodstream forms of trypanosomes. It contains two twin CX_9C motifs and mediates import of both presequence-containing and mitochondrial carrier proteins. While the precise function of TbTim15 in mitochondrial protein import is unknown, our results are consistent with the notion that it may function as an import receptor for the non-canonical trypanosomal TIM complex.

KEYWORDS
Cx9X motifs, intermembrane space, mitochondrial protein import, TIM complex, Trypanosomes

1 | INTRODUCTION

Mitochondria or mitochondria-derived organelles are hallmarks of eukaryotes and fulfill various essential functions (van der Bliek et al., 2017). Due to their endosymbiotic origin, mitochondria contain their own genome, which, however, only encodes for a small fraction of mitochondrial proteins (Roger et al., 2017). Thus, >95% of all mitochondrial proteins are encoded in the nucleus, synthesized in the cytosol, and subsequently imported into mitochondria (Hansen & Herrmann, 2019; Wiedemann & Pfanner, 2017). Most experimental studies on mitochondrial protein import have been done in the yeast *Saccharomyces cerevisiae* and in mammals, both of which belong to

the eukaryotic supergroup Opisthokonta (Burki et al., 2020). These studies have shown that the majority of proteins enter mitochondria through a common entry gate, the translocase of the outer mitochondrial membrane (TOM; Eaglesfield & Tokatlidis, 2021; Gupta & Becker, 2021). Depending on distinct targeting signals, the imported substrates are then sorted to their submitochondrial destination. Yeast and most other eukaryotes, in which mitochondrial protein import has been investigated, have two translocases of the inner mitochondrial membrane (TIM), the TIM22 and TIM23 complexes (Fukasawa et al., 2017; Žárský & Doležal, 2016). The TIM22 complex, also referred to as the carrier translocase, mediates the insertion of proteins into the inner mitochondrial membrane (IM) which have multi-spanning transmembrane domains (TMDs), such as mitochondrial carrier proteins (MCPs; Ferramosca & Zara, 2013; Zimmermann & Neupert, 1980). The TIM23 complex, also termed presequence translocase, imports presequence-containing precursor proteins across or into the IM (Hansen & Herrmann, 2019; Marom et al., 2011; Schulz et al., 2015), which represent 60%–70% of all mitochondrial proteins (Vögtle et al., 2009). To that end, TIM23 associates with the matrix-exposed presequence translocase-associated motor (PAM). The yeast PAM consists of five essential components (Craig, 2018; Schulz et al., 2015): the mitochondrial heat shock protein 70 (mHsp70; Horst et al., 1997; Kang et al., 1990); the J-domain containing co-chaperones Pam18 (D'Silva et al., 2003; Truscott et al., 2003) and Pam16 (Frazier et al., 2004); Tim44 which tethers mHsp70 to TIM23 (Banerjee et al., 2015); and the nucleotide exchange factor Mge1 (Laloraya et al., 1994, 1995; Schneider et al., 1996).

During the last decade, the unicellular parasite *Trypanosoma brucei*, a member of the eukaryotic supergroup of the Discoba (Burki et al., 2020), has emerged as an experimentally highly accessible, non-opisthokont model system for mitochondrial biology. Studies on mitochondrial protein import in *T. brucei* have shown that the trypanosomal import systems are highly diverged compared to other eukaryotes (Harsman & Schneider, 2017; Schneider, 2018, 2020). Accordingly, the trypanosomal TOM complex, referred to as atypical TOM (ATOM), shares only two of its seven subunits with other eukaryotes (Mani et al., 2015, 2016, 2017). However, the largest differences to other eukaryotes concern the IM translocases. Epitope-tagged import substrates, stalled within either the presequence translocase or the carrier translocase, were used to show that *T. brucei* has a single TIM complex only. This single TIM, with minor compositional variations, can import presequence-containing proteins as well as MCPs (Harsman et al., 2016). It consists of the essential integral IM proteins TbTim17, TbTim62, TbTim42, and a medium chain length acyl-CoA dehydrogenase (ACAD; Figure 1a; Harsman et al., 2016; Singha et al., 2008, 2012, 2015). TbTim17 is an ortholog of Tim22, the pore-forming subunit of the TIM22 complex in yeast (Fukasawa et al., 2017; Pyrihová et al., 2018; Žárský & Doležal, 2016). It is the only integral membrane TIM subunit that shares homology with components of the IM translocase of other eukaryotes (Harsman et al., 2016; Singha et al., 2012). Furthermore, the single TIM complex is associated with six intermembrane space (IMS)-localized small Tim chaperones, termed Tim8-13, Tim9, Tim10, TbTim11, TbTim12, and TbTim13 (Gentle et al., 2007; Harsman et al., 2016; Wenger et al., 2017). The trypanosomal small Tims show homology to small Tim chaperones of other eukaryotes that specifically interact with the TIM22 complex and escort hydrophobic substrate across the aqueous IMS. Two additional integral membrane proteins, the proteolytically inactive rhomboid-like proteins TimRhom I and TimRhom II, are associated with the trypanosomal TIM complex. Interestingly, they appear to be selectively required for import of presequence-containing proteins (Harsman et al., 2016). Finally, import of presequence-containing proteins requires the trypanosomal TIM complex to associate with an unconventional PAM module (von Känel et al., 2020). The trypanosomal PAM contains orthologs of mHsp70 (TbmHsp70) and Mge1 (TbMge1) and the kinetoplastid-specific J-domain protein TbPam27 (von Känel et al., 2020) but lacks homologs of yeast Pam18, Pam16, and Tim44.

Using tagged TbPam27 as the bait in a quantitative co-immunoprecipitation (CoIP) experiment, we discovered a new subunit of the trypanosomal TIM complex, which was termed TbTim15. TbTim15 was also enriched in pull-down experiments of three other TIM subunits (Harsman et al., 2016; von Känel et al., 2020). Furthermore, in these experiments, we also discovered another protein that seems to be closely associated with the IM import machinery. We refer to this protein as putative TbTim20. TbTim15 is an IMS-localized TIM complex-associated protein that mediates import of presequence-containing and of MCPs. In contrast, putative TbTim20 appears to have a non-essential function under the tested conditions.

2 | RESULTS

2.1 | Identification of novel trypanosomal TIM or PAM subunit candidates

TbPam27, aside from TbmHsp70, is the first experimentally analyzed subunit of the trypanosomal PAM. It is closely associated with the single TIM complex, when it translocates presequence-containing proteins (Harsman et al., 2016; von Känel et al., 2020). To identify new putative TIM or PAM subunits, we used a tetracycline-inducible, C-terminally myc-tagged TbPam27 (TbPam27-myc) as the bait in a CoIP experiment employing stable isotope labelling by amino acids in cell culture (SILAC). (Note: If not indicated otherwise, all experiments described in this study have been done in procyclic stage cells). Subsequently, the eluted proteins were analyzed by quantitative mass spectrometry (MS) in triplicate experiments to determine protein abundance ratios.

The resulting TbPam27-myc SILAC CoIP eluate contained 74 mitochondrial proteins (Peikert et al., 2017) that were enriched more than fivefold when compared to uninduced cells (Figure 1b, Table S1). Importantly, all six essential integral membrane components of the presequence-translocase form of the TIM complex (Harsman et al., 2016) were among the top 10 enriched

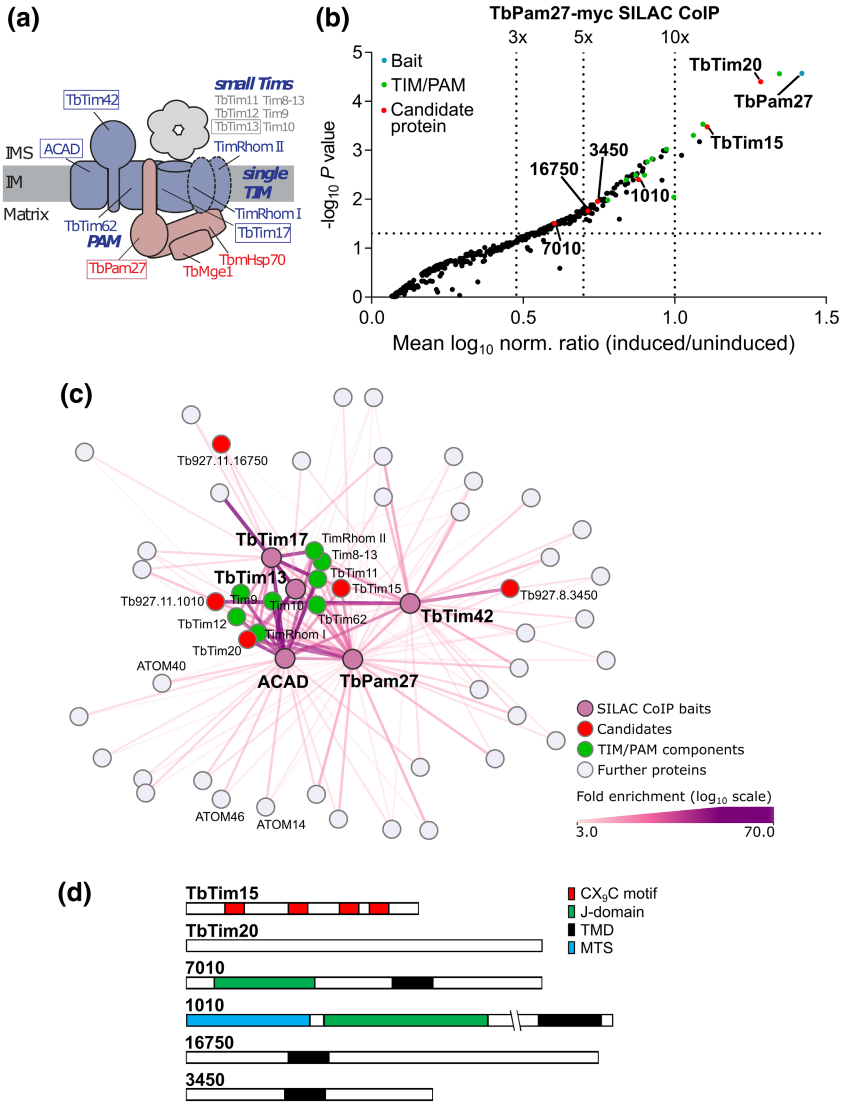

FIGURE 1 TbPam27-myc SILAC CoIP reveals new TIM and PAM subunit candidates: (a) Scheme of the subunit composition of the single trypanosomal inner membrane translocase. All shown subunits are essential for growth. Blue, TIM core subunits; gray, small Tim complexes; red, PAM subunits. Broken lines indicate selective association with the presequence translocase. Proteins utilized as baits in the pulldown experiments used to generate the protein–protein interaction network shown in (c) are boxed. (b) Volcano plot depicting mitochondrial proteins detected in SILAC-based quantitative mass spectrometry analysis of TbPam27-myc CoIPs. Y-axis depicts adjusted p-value ($-\log_{10}$). Differentially labeled uninduced and induced cells were mixed and subjected to CoIP. The experiment was done in triplicate. The vertical dotted lines in the volcano plot indicate the specified enrichment factors. The horizontal dotted line indicates an adjusted *p* value of 0.05. The bait TbPam27 is highlighted in blue, TIM and PAM components in green and candidate proteins chosen for experimental analysis in red. (c) Edge-weighted protein–protein interaction network generated using Cytoscape (version 3.9). Network depicts proteins enriched more than threefold in at least two of the SILAC CoIPs using TbPam27, TbTim17, TbTim42, ACAD, and TbTim13 as the baits (baits shown in pink). Candidates chosen for experimental analysis are shown in red, TIM and Pam subunits in green and further proteins in gray. The fold enrichment is indicated by the line-width and color intensity of the connecting lines. Candidate 7010 was enriched in the TbPam27 SILAC CoIP, but not in the other analyzed TIM subunit CoIPs. Therefore, it is not part of the protein interaction network. (d) Schematic to scale representation of candidate proteins. In silico predicted domains are indicated.

mitochondrial proteins (all more than ninefold) following the bait. Furthermore, the six trypanosomal small Tim chaperones (Gentle et al., 2007; Harsman et al., 2016; Wenger et al., 2017) were all more than sixfold enriched (Figure 1b, Table S1). To identify new putative TIM or PAM complex subunits, we generated an edge-weighted protein–protein interaction network using Cytoscape (version 3.9; Shannon et al., 2003). For this analysis, we considered the TbPam27 SILAC CoIP and the previously published SILAC CoIPs of the TIM core subunits (TbTim17, Harsman et al., 2016, TbTim42 Harsman et al., 2016, ACAD von Känel et al., 2020) as well as the small Tim protein TbTim13 (Harsman et al., 2016; Figure 1a,c). The network contains proteins that were enriched more than threefold in at least two of these SILAC CoIP experiments (Figure 1c). Of the resulting cluster, we chose five proteins, Tb927.2.4445, Tb927.11.1620,

Tb927.11.1010, Tb927.11.16750, and Tb927.8.3450, that have been especially highly enriched (more than fivefold) in the TbPam27 SILAC CoIP (Figure 1b,c, Table S1), for further experimental analysis. We named Tb927.2.4445 and Tb927.11.1620, TbTim15 and putative TbTim20, respectively, according to their predicted molecular weights. The remaining candidates will be referred to as 1010, 16750, and 3450.

Of the five candidates, only TbTim15 and putative TbTim20 were enriched in a SILAC pull-down experiment of a tagged presequence-containing substrate that is stuck in the TIM complex (Figure S1A; Harsman et al., 2016). Whereas none of them, with the possible exception of TbTim15, which was not detected in the SILAC pull down, was recovered with a truncated tagged MCP that is stalled in the TIM complex (Harsman et al., 2016). To find out whether TbTim15 is part of the active carrier translocase, we repeated this experiment (Figure S1B; Harsman et al., 2016). The result showed that TbTim15 was indeed co-purified with the stalled MCP as revealed by immunoblots using a newly produced anti-TbTim15 antibody (Figure S2A). Thus, TbTim15 is the only candidate, which is part of both, the active presequence (Harsman et al., 2016) and the active carrier translocase (Figure S1).

Finally, we added Tb927.8.7010 to our candidate list, even though it was enriched only fourfold in the TbPam27-myc SILAC CoIP, because it was highly enriched in the CoIP of the active presequence translocase but not associated with the carrier translocase (Figure 1b, Figure S1A).

The domain structure of all six new putative TIM or PAM subunits were analyzed in silico (Figure 1d). TbTim15 contains four CX_9C motifs (C=cysteine, X=any amino acid but cysteine), which are typically found in IMS proteins (Longen et al., 2009; Peikert et al., 2017). In the AlphaFold structure prediction of TbTim15 (Figure S2B; Wheeler, 2021), each twin CX_9C motif is positioned in a loop, which would allow for the formation of two intramolecular disulfide bridges. Such disulfide bridges are known to trap the protein in the IMS. In both yeast and *T. brucei*, the import of proteins into the IMS depends on orthologs of Erv1 (Allen et al., 2005; Ceh-Pavia et al., 2020; Peikert et al., 2017). Moreover, in *T. brucei*, the MICOS subunit TbMic20 has also been implicated in import of IMS proteins (Kaurov et al., 2018, 2022). Interestingly, in previous quantitative proteomics studies, TbTim15 was shown to be downregulated 3.65-fold upon TbErv1 RNAi (Peikert et al., 2017) and 2.36-fold upon TbMic20 RNAi (Kaurov et al., 2018). We confirmed these findings by following the steady-state levels of TbTim15 in previously generated TbErv1 (Peikert et al., 2017) and TbMic20 (Kaurov et al., 2018) RNAi cell lines over several days of induction (Figure 2a,b). Thus, TbTim15 most likely is an IMS protein.

For putative TbTim20, none of various online prediction tools (Blum et al., 2021; Emanuelsson et al., 2007; Gabler et al., 2020; Krogh et al., 2001; Letunic et al., 2021) recovered any recognizable domains (Figure 1d). 7010, 1010, 16750, and 3450, all contain a single predicted TMD (Krogh et al., 2001) and for 1010, an N-terminal mitochondrial targeting signal (MTS) was predicted (Claros & Vincens, 1996). In addition, 7010 and 1010 contain predicted

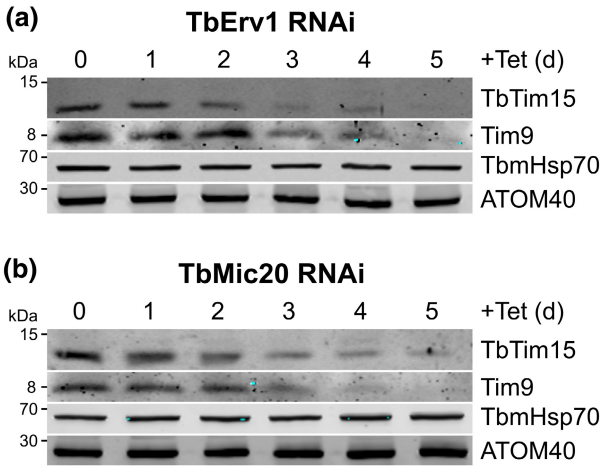

FIGURE 2 TbTim15 is an intermembrane space protein: Immunoblot analysis of steady-state protein levels of TbTim15 in (a) TbErv1 and (b) TbMic20 RNAi background over 5 days of induction. Tim9, TbmHsp70, and ATOM40 were used as markers for intermembrane space, matrix, or outer membrane proteins, respectively.

J-domains at their N termini (Figure 1d; Blum et al., 2021; Letunic et al., 2021).

Basic local alignment tool (BLAST; Agarwala et al., 2016) and secondary structure similarity analysis by HHPred (Gabler et al., 2020) showed that all candidates are conserved among kinetoplastids. TbTim15, putative TbTim20, 16750, and 3450 show no obvious similarities to proteins in *S. cerevisiae* or humans. For 7010 and 1010, the similarities detected to proteins of other species were limited to the respective J-domains.

2.2 | All candidates are mitochondrial integral membrane or partially membrane-associated proteins

All our candidate proteins are components of the previously defined mitochondrial importome (Peikert et al., 2017) and all, except 3450, are components of an earlier identified cluster of IM proteins (Niemann et al., 2013). To confirm the mitochondrial localization of the six candidates experimentally, cell lines allowing the inducible ectopic expression of C-terminally HA-tagged versions of the proteins were generated (Figure S2C illustrates the specificity of the anti-HA antibody). These cell lines were subjected to digitonin extractions allowing the separation of a mitochondria-enriched pellet from a cytosolic fraction. As shown in Figure S3, all HA-tagged candidates co-fractionate with the mitochondrial marker ATOM40 in such an experiment. These findings were confirmed by immunofluorescence microscopy analysis, in which the HA-tagged candidates co-localized with ATOM40 (Figure S4). Moreover, alkaline carbonate extractions of the mitochondria-enriched pellets showed that, except for the IMS-localized TbTim15-HA, all candidates were predominantly recovered in the pellet together with ATOM40. This suggests they are integral membrane proteins

or strongly membrane-associated proteins (Figure S3). However, while TbTim15-HA was mainly found in the soluble fraction, a small portion was also found in the pellet suggesting TbTim15 is at least partially associated with a mitochondrial membrane. The pellet portion of TbTim15 does not represent an insoluble protein aggregate as it could be solubilized in 1% Triton X-100 (Figure S3). These results suggest that a fraction of the IMS-localized TbTim15 is tightly membrane-associated.

Putative TbTim20 is part of the IM proteome (Niemann et al., 2013), but it has no predicted TMD (Figure 1c). The fact that it was recovered in the pellet fraction of an alkaline carbonate extraction (Figure S3) suggests that it is closely associated with the IM, despite the absence of a predicted TMD. Moreover, as in the case of TbTim15, the pellet can be solubilized with Triton X-100 indicating it is not an insoluble protein aggregate. Concerning 7010, 1010, and 16750, previous proteomic analyses (Niemann et al., 2013; Peikert et al., 2017), the predicted TMDs (Figure 1c), the experimental data in Figures S3 and S4 taken together suggest that they all are integral IM proteins. 3450 is a mitochondrial membrane protein that was not detected in the abundance profiling that led to the IM proteome (Niemann et al., 2013).

2.3 | TbTim15 and putative TbTim20 are associated with the TIM complex

To confirm that our selected candidates are associated with the TIM complex and interact with TbPam27, the HA-tagged candidate proteins were used as baits in anti-HA CoIP experiments. The resulting immunoblots were probed with anti-HA antibodies and the previously established antisera against the TIM subunits TbTim17, TimRhom I, as well as the small Tim chaperone Tim9 (Harsman et al., 2016). Furthermore, newly produced antibodies recognizing TbPam27 and TbTim15 were used (for validation of antibodies, see Figure S2A,D). In line with their central position in the TIM complex protein interaction network (Figure 1b), TbTim15-HA and putative TbTim20-HA CoIPs efficiently recovered TbPam27, as well as all tested TIM subunits (Figure 3a). Thus, we conclude that TbTim15 and putative TbTim20 are associated with TbPam27 and the entire TIM complex.

In the 7010-HA CoIP (Figure 3a), TbPam27 was found to be enriched, as expected from the TbPam27-myc SILAC CoIP (Figure 1b, Table S1) confirming the reciprocal interaction between the two proteins. 7010 was also detected in pulldown when using the stuck precursor but not the stuck carrier substrate as a bait (Figure S1A). However, it was not enriched in any pulldown using tagged TIM subunits, and thus, does not show up in the TIM complex protein interaction network (Figure 1c). Therefore, 7010 seems to be only recruited to the TIM complex, when a presequence-containing substrate is being imported.

CoIP experiments in which 1010-HA, 16750-HA, and 3450-HA were used as the baits, did not enrich for TbPam27 or any other of the tested TIM subunits (Figure 3a). This is surprising because all of them were enriched more than fivefold in the TbPam27 SILAC CoIP (Figure 1b, Table S1) and significantly enriched in more than one TIM subunit SILAC CoIP performed in previous studies (Figure 1c). The reason for this is unclear but 16750 and 3450 localize to the periphery of the TIM complex protein interaction network indicating a weaker association with the TIM complex (Figure 1c). Moreover, it is possible that the HA-tag interferes with protein–protein interactions.

Because they are the only candidates clearly associated with TbPam27 and the TIM complex, we focused on TbTim15 and putative TbTim20 for further analysis. Blue native (BN)-PAGE, which allows the size separation of multiprotein complexes under native conditions, showed that TbTim15, putative TbTim20-HA, and TbPam27 are all present in high molecular weight (HMW) complexes (Figure 3b, Figure S2E). Interestingly, while TbTim15 is present in two distinct complexes of approximately 700 kDa, the complexes formed by TbPam27 and putative TbTim20 overlap with the ones containing TbTim15, but are highly heterogenous.

In summary, these results show that TbTim15 and putative TbTim20 are present in the PAM/TIM/small Tim supercomplex.

2.4 | TbTim15 is essential for mitochondrial protein import

To learn more about the functions of TbTim15, putative TbTim20, 7010, 1010, 16750, and 3450, inducible RNAi cell lines were established. Figure 4a shows that RNAi-induced knockdown of TbTim15 led to a strong growth retardation after 2 days of induction and a complete growth arrest at later timepoints. Knockdown of putative TbTim20, 7010, and 1010 does not affect normal growth. Thus, putative TbTim20, within the limits of RNAi analysis, is not essential for normal growth even though it is clearly associated with both TIM and PAM subunits (Figures 1b,c and 3). Finally, RNAi-mediated ablation of 16750 and 3450 causes a slight reduction in growth rates between 3 and 4 days after RNAi induction (Figure 4a).

Next, we tested whether TbTim15, 16750, and 3450, for which RNAi induction caused a change in the growth rate, are involved in mitochondrial protein import. To that end, we analyzed steady-state levels of cytochrome c oxidase subunit 4 (CoxIV) in whole cell extracts of the respective RNAi cell lines (Figure 4b). Accumulation of the unprocessed precursor of CoxIV in the cytosol, which still contains its N-terminal presequence, is a hallmark of a general mitochondrial protein import defect (Harsman et al., 2016; Mani et al., 2015; von Känel et al., 2020). In the TbTim15 RNAi cell line, but not in the other two tested cell lines, we observed an accumulation of CoxIV precursor after 2 days of induction, which corresponds to the onset of the growth phenotype (Figure 4a).

Digitonin fractionation showed that while the mature form of CoxIV almost exclusively co-fractionated with the mitochondrial marker, the CoxIV precursor was found in the cytosolic fraction (Figure 4c), as would be expected in the case of an import defect.

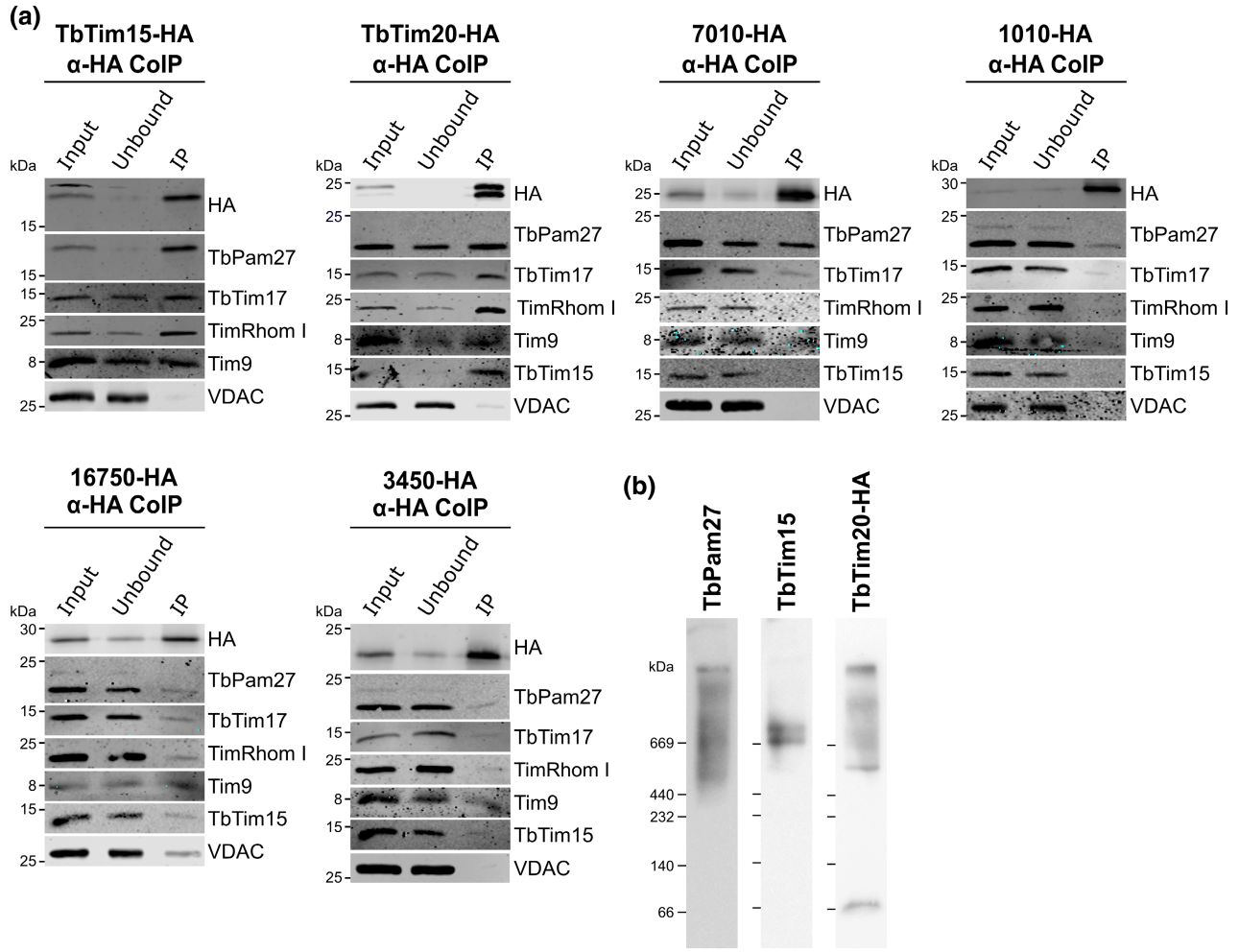

FIGURE 3 TbTim15 and putative TbTim20 are associated with the TIM complex: (a) Cell lines expressing the C-terminally HA-tagged candidate proteins were subjected to co-immunoprecipitation (CoIP) experiments. 5% of mitochondria-enriched fractions (Input), 5% of unbound proteins (Unbound), and 100% of the final eluates (IP) were analyzed by immunoblotting. The immunoblots were probed with anti-HA antibodies, antisera against TbPam27 and TbTim15, as well as the TIM subunits TbTim17, TimRhom I, the small Tim Tim9, and the voltage-dependent anion channel VDAC. All CoIP experiments have been done at least twice. (b) Blue native (BN)-PAGE analysis of TbPam27, TbTim15, and putative TbTim20-HA complexes in mitochondria-enriched fractions. Blots were probed with anti-TbPam27, anti-TbTim15, and anti-HA antibodies. For control of specificity of anti-TbPam27 and anti-TbTim15 antibodies, see Figure S2D.

FIGURE 4 TbTim15 is essential for mitochondrial protein import: (a) Growth curves of uninduced (−Tet) and induced (+Tet) RNAi cell lines. Inset in the growth curve of the TbTim15 RNAi cell line shows immunoblot of whole cell extracts of uninduced and two days induced RNAi cells. The blot was probed with anti-TbTim15 antibody and EF1a as loading control. Insets in remaining growth curves show northern blots of total RNA extracted from uninduced and 2-day induced cells, which were probed for the corresponding mRNAs. Ethidium bromide-stained ribosomal RNAs (rRNAs) serve as loading controls. (b) Immunoblot analysis of steady-state protein levels of cytochrome oxidase subunit 4 (CoxIV) in whole cell extracts of the indicated RNAi cell lines. CoxIV precursor (P) and mature form (M) are indicated. Elongation factor 1 alpha (EF1a) serves as loading control. (c) Immunoblot analysis of total TbTim15 RNAi cells (T), as well as digitonin-extracted, mitochondria-enriched (M), and soluble cytosolic (S) fractions. Blots were probed with anti-CoxIV antibodies and antisera against VDAC and EF1a, which serve as mitochondrial and cytosolic markers, respectively. (d) Immunoblot analysis of steady-state levels of the OM protein ATOM69, the IMS proteins Tim9 and cytochrome C (Cyt C), the IM protein MCP5, and the matrix proteins REAP1, TbmHsp60, LipDH, and TbmHsp70 in whole cell extracts of the TbTim15 RNAi cell line. (e) Growth curve of uninduced (−Tet) and induced (+Tet) bloodstream form (BSF) γL262 cell lines, containing normal amounts of kDNA, ablating TbTim15. Inset shows immunoblot of whole cell extracts of uninduced and 2-day induced RNAi cells. The blot was probed with anti-TbTim15 antibody and EF1a as loading control. (f) Left: BN-PAGE analysis of the TIM complex in cell lines expressing TbTim17-HA in the background of TbTim15 RNAi. The resultant immunoblot was probed with anti-HA antibody. Coomassie-stained gel section (Coom.) serves as loading control. Right: Densitometric quantification of the BN-PAGE. Green bars correspond to the mean of three independent biological replicates. Levels in uninduced cells were set to 100%. n.s., not significant, as calculated by an unpaired two-sided *t*-test. All growth curves have been done at least twice.

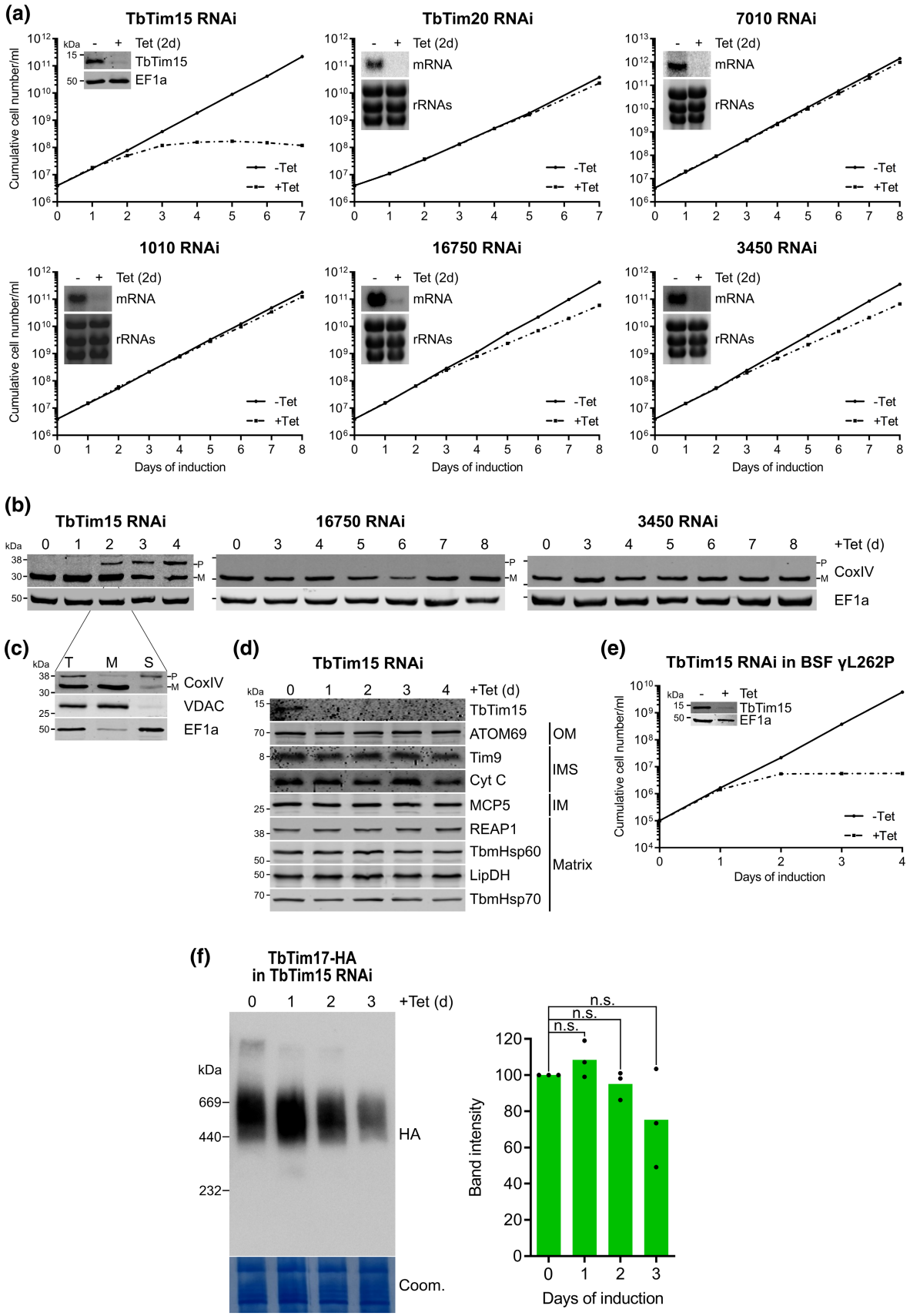

In an effort to detect further substrates of TbTim15, we analyzed the steady-state levels of a panel of mitochondrial proteins on immunoblots before and after RNAi-mediated depletion of TbTim15 (Figure 4d). However, neither a change in their levels nor precursor accumulation was observed for any of the tested proteins including the IMS-localized Tim9 and cytochrome C.

Moreover, immunofluorescence microscopy of ATOM40- and Mitotracker-stained TbTim15 RNAi cells confirmed that the general mitochondrial morphology remained unchanged and that the mitochondrial membrane potential was still intact at the timepoint the import phenotype becomes apparent (Figure S5).

Trypanosoma brucei has a complex life cycle and alternates between an insect vector, the Tsetse fly, and a mammalian host. In the procyclic form (PCF) in the fly, the mitochondrion is capable of oxidative phosphorylation (OXPHOS). In contrast, mitochondria of the bloodstream form (BSF) lack the respiratory complexes, except for the ATP-synthase, which functions in reverse (Schnaufer et al., 2002). However, both the PCF and the BSF depend on mitochondrial protein import (Cristodero et al., 2010). Results obtained with an inducible TbTim15 RNAi cell line of the BSF strain γL262P (Dean et al., 2013) showed that TbTim15, as expected for a general import factor, is also essential for normal growth of the γL262P and very likely also of "wildtype" BSF trypanosomes (Figure 4e).

TbTim15 could be required either for the assembly of the TIM complex or directly mediate protein import. BN-PAGE analysis of a TbTim15 RNAi cell line expressing a C-terminally HA-tagged version of the TIM core subunit TbTim17 showed that the formation and stability of the TIM complex was not significantly affected for at least 3 days after RNAi induction (Figure 4f). This suggests that TbTim15 does not mediated TIM complex assembly and instead has a more direct role in mitochondrial protein import.

2.5 | TbTim15 is required to stall the presequence and the carrier pathway intermediates

Using artificial import substrates that can be arrested in either the presequence or the MCP pathway, it could be shown that some TIM subunits are specifically associated with the active presequence translocase but absent from the MCP translocase form of the single trypanosomal TIM complex (Harsman et al., 2016). The presequence pathway intermediate is formed by the expression of a C-terminally tagged presequence-containing substrate that is fused to dihydrofolate reductase (DHFR). Addition of the folate-analog aminopterin (AMT) prevents import of the C-terminal part of the chimeric protein as it tightly binds to the DHFR moiety. This results in a substrate that is stuck in the import channels across both the OM and the IM. The MCP pathway intermediate is formed by expression of truncated version of a tagged MCP that lacks the two N-terminal TMDs, which causes its accumulation in the carrier translocase. Formation of the two import intermediates can be monitored by BN-PAGE analysis.

To find out whether TbTim15 can be assigned to either the presequence or the carrier pathway, we expressed the two modified import substrates in the background of TbTim15 RNAi. Figure 5 shows that after 2 days of RNAi induction, at the onset of the growth phenotype (Figure 4a) and at a time when the TIM complex was still intact (Figure 4f), the formation of both substrate-containing translocase complexes was significantly reduced. These findings demonstrate that TbTim15 is required for the formation of both, the presequence and the carrier pathway intermediate. Hence, it is probably involved in both pathways. These results also suggest that TbTim15 is rather a component of the TIM complex than of the PAM module. Importantly, the same assay had previously been used to show that TbPam27, as expected for a PAM subunit, is selectively required for the formation of the presequence but not the carrier pathway intermediate (von Känel et al., 2020).

3 | DISCUSSION

Trypanosoma brucei contains a non-canonical single TIM complex that mediates the import of presequence-containing proteins and of MCPs (Harsman et al., 2016). To translocate presequence-containing proteins, the TIM complex associates with an unusual PAM that contains the kinetoplastid-specific TbPam27 (von Känel et al., 2020). Here, we used TbPam27 as the bait in a SILAC CoIP experiment, which together with a re-analysis of previously published SILAC CoIPs of various TIM complex subunits, revealed six new candidates for TIM subunits or TIM-associated proteins (Figure 1b,c). These candidates are all kinetoplastid-specific, mitochondrial proteins (Figures S3 and S4; Peikert et al., 2017). RNAi-mediated depletion of these proteins showed that only TbTim15 is essential for normal growth and that depletion of the other five candidates either did not or only marginally impede growth of PCF trypanosomes (Figure 4a).

Thus, we focused our studies mainly on TbTim15. It contains twin CX_9C motifs (Figure 1d, Figure S2B) that are characterized by two α-helices forming an antiparallel α-hairpin that is covalently paired by two disulfide bridges (Modjtahedi et al., 2016). Twin CX_9C motif-containing proteins generally localize to the IMS. This is also the case for TbTim15, which requires the IMS import factors TbErv1 (Peikert et al., 2017) and TbMic20 (Kaurov et al., 2018) for its import (Figure 2). Twin CX_9C motif-containing proteins perform diverse mitochondrial functions. Many are involved in OXPHOS as non-catalytic subunits or assembly factors of complex I and complex IV of the respiratory chain. Others regulate mitochondrial morphology as MICOS subunits or are involved in maintaining lipid homeostasis (Modjtahedi et al., 2016). Whereas most twin CX_9C motif-containing proteins have a single twin CX_9C motif, TbTim15 contains two. Other examples for proteins with quadruple CX_9C motifs include the mammalian complex I subunit NDUFA8 (Szklarczyk et al., 2011) and the mammalian MICOS subunit Mix14 (Khalimonchuk & Winge, 2008).

Three lines of experimental evidence indicate that the trypanosomal TbTim15 functions in mitochondrial protein import: (i) While not having an obvious predicted TMD (Figure S3), TbTim15 is constitutively associated with the single PAM/TIM/small TIM supercomplex (Figures 1b,c and 3, Figure S1), regardless of whether it is engaged in import of presequence-containing proteins or MCPs (Figure S1); (ii) depletion of TbTim15 results in the accumulation of uncleaved precursor of CoxIV (Figure 4b,c), and prevents the formation of import-arrested substrates in both the presequence as well as the carrier translocases (Figure 5a,b); and (iii) TbTim15 is essential

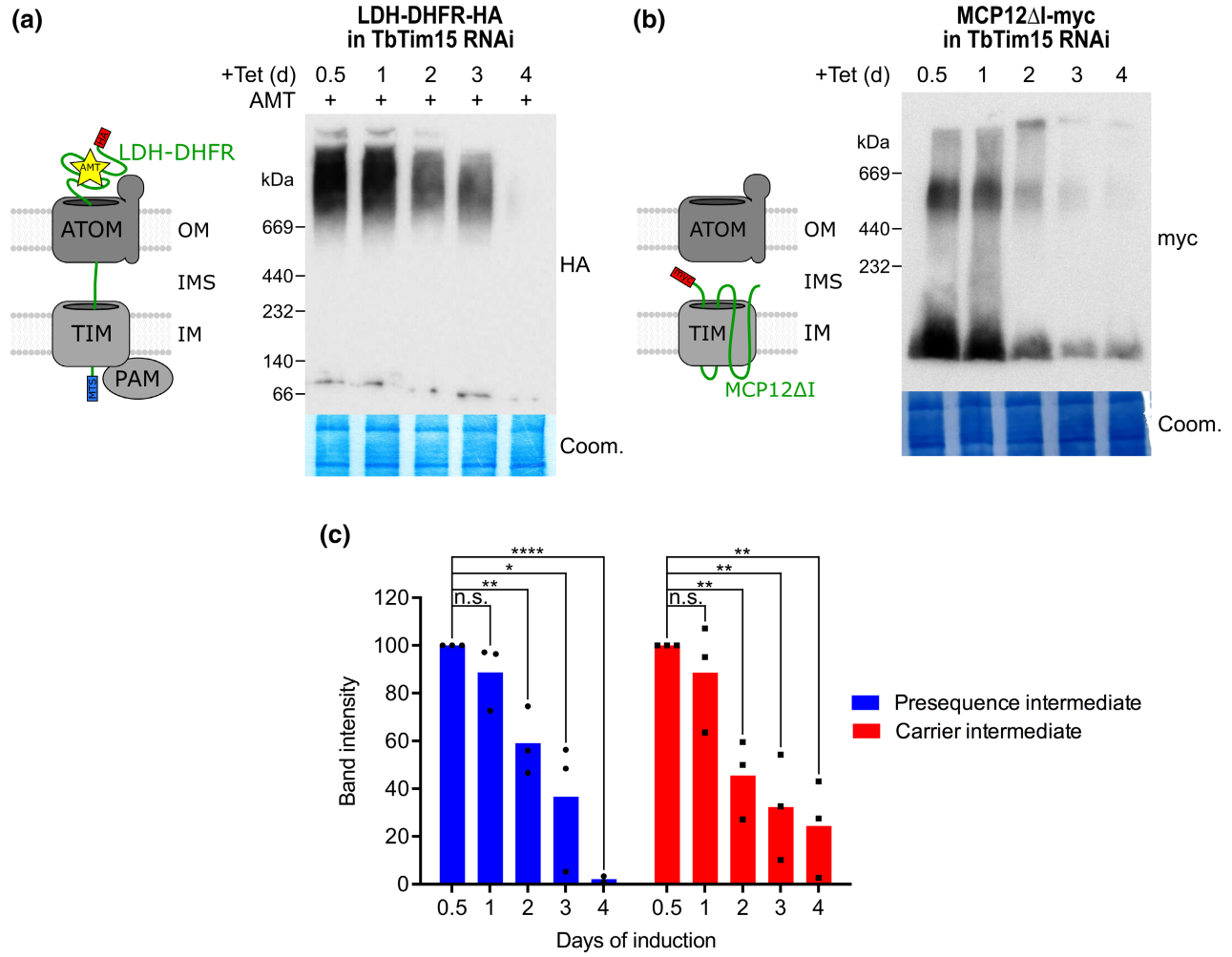

FIGURE 5 TbTim15 is required to stall the presequence and the carrier pathway intermediates: (a) Left: Schematic representation of the stalled presequence pathway intermediate induced in vivo by expression of the LDH-DHFR-HA fusion protein in the presence of aminopterin (AMT). Right: BN-PAGE analysis of the presequence pathway intermediate in mitochondria-enriched fractions of cells expressing LDH-DHFR-HA in the background of TbTim15 RNAi. Cells were induced (+Tet) for 0.5–4 days (d) and grown in the presence of AMT for 0.5 days prior to the experiment. The resultant immunoblot was probed with anti-HA antibody. Coomassie-stained gel section (Coom.) serves as loading control. (b) Left: Schematic representation of the import-arrested carrier intermediate induced in vivo by the expression of the truncated myc-tagged mitochondrial carrier protein 12 (MCP12ΔI-myc). Right: BN-PAGE analysis of the carrier intermediate in mitochondria-enriched fractions of cells expressing MCP12ΔI-myc in the background of TbTim15 RNAi. Cells were induced (+Tet) for 0.5–4 days (d). The resultant immunoblot was probed with anti-myc antibody. Coom. serves as loading control. The red boxes indicate the HA- or myc epitope tags, respectively. (C) Densitometric quantification of the BN-PAGE signals to compare the amount of stalled LDH-DHFR-HA (as shown in a) and MCP12ΔI-myc (as shown in b) in TbTim15 RNAi background in the respective high molecular weight complexes. The levels after 0.5 days of RNAi induction were set to 100%. Blue (presequence intermediate) and red (carrier intermediate) bars represent the mean of three independent biological replicates, respectively. n.s., not significant, **p*-value < 0.05, ***p*-value < 0.01, *****p*-value < 0.0001, as calculated by an unpaired two-tailed *t*-test.

for normal growth of both the PCF and the BSF of trypanosomes (Figure 4a,e). BSF parasites, except for the ATP synthase, lack the respiratory complexes, and therefore, are not capable of OXPHOS (Fenn & Matthews, 2007). This indicates that the role of TbTim15, unlike many twin CX_9C motif-containing proteins in other organisms, cannot be restricted to OXPHOS. Rather it must be involved in a more general process that is essential in both life cycle stages, such as mitochondrial protein import.

Presently, the precise function of TbTim15 in mitochondrial protein import is unknown. There are many possibilities, including that it may function as an IMS-localized chaperone, such as the six previously identified small TIM proteins (Smith et al., 2018; Wenger et al., 2017), or as a receptor for substrates of the TIM complex. Intriguingly, there is a well-studied twin CX_9C motif-containing protein, termed Mia40 that is involved in mitochondrial protein import in yeast and mammals. Mia40 together with Erv1 forms a disulfide relay, which imports small cysteine motif-containing proteins into the IMS. In this relay, Mia40 performs two distinct functions: It serves as a receptor for its substrates, and it oxidizes their cysteines (Peleh et al., 2016). The electrons liberated in the oxidation are

subsequently transferred to cytochrome c by the sulfhydryl oxidase Erv1. While Erv1 and Mia40 are conserved in most eukaryotes, *T. brucei* and its relatives lack a Mia40 ortholog (Basu et al., 2013). It is therefore unclear whether the trypanosomal Erv1 directly oxidizes IMS proteins or, as has been suggested in plants (Peleh et al., 2017), whether Mia40 has been replaced by another protein (Allen et al., 2008; Turra et al., 2021).

It would be interesting to investigate whether TbTim15 could, at least partially, take over the function of the lacking Mia40. In yeast, the essential receptor function of Mia40 is mediated by the pocket formed by the twin CX_9C motif, whereas the oxidase activity requires the CPC motif in the N-terminal domain of the protein (Peleh et al., 2016). TbTim15 lacks a CPC motif, and therefore, likely has no oxidase activity. Yet, it does have two twin CX_9C motifs (Figure 1d, Figure S2B), which could form pockets recognizing imported proteins. However, in contrast to yeast Mia40, TbTim15 is associated with the TIM complex (Figures 1b,c and 3) and involved in both the presequence and the MCP import pathway (Figure S1, Figure 5). This suggests that, should TbTim15 indeed be an import receptor, it would recognize different or a wider range of substrates than Mia40, including presequence-containing as well as MCPs. Intriguingly, it has recently been proposed that also yeast Mia40 might be involved in import of non-typical substrates (Okamoto et al., 2014; Petrungaro et al., 2015; Wrobel et al., 2013). However, an immunoblot analysis of the changes in the steady-state levels of eight mitochondrial proteins after depletion of TbTim15 failed to reveal further TbTim15 substrate candidates (Figure 4d) suggesting it may have a rather narrow substrate specificity. Trypanosomes lack a Tim50 ortholog, which serves as an import receptor for the TIM23 complex of yeast and mammals, and no other receptor subunit has been identified (Harsman et al., 2016). Contrary to depletion of any of the integral membrane TIM subunits (Harsman et al., 2016), lack of TbTim15 seems to not directly interfere with the assembly or the stability of the TIM complex (Figure 4f). This is reminiscent of the two receptors ATOM46 and ATOM69 of the ATOM complex of trypanosomes (Mani et al., 2015), and of the Tom20 and Tom70 receptors of the yeast and mammalian TOM complexes (Lithgow et al., 1994), whose absence does not affect the integrity of the (A) TOM complexes.

It has recently been suggested that the IMS-localized trypanosomal protein TbTim54, as TbTim15, is associated with the trypanosomal TIM complex (note that despite its name, TbTim54 is not related to the yeast TIM22 complex subunit Tim54; Singha et al., 2012, 2021). In contrast to TbTim15, it was proposed that TbTim54 mediates the assembly of the TIM complex and the import of at least a subset of MCPs (Singha et al., 2021). However, unlike expected for a TIM complex assembly factor, knockdown of TbTim54 only marginally affects cell growth (Singha et al., 2012). Moreover, TbTim54 was neither enriched in any of the SILAC pulldown of the core TIM subunits (TbTim17, TbTim42, ACAD) (Harsman et al., 2016; von Känel et al., 2020), the small TIM protein TbTim13 (Harsman et al., 2016), nor the PAM subunit TbPam27 tested in the present study (Table S1). Thus, the question how closely TbTim54 is associated with the trypanosomal TIM complex remains open at present.

In summary, we show that TbTim15 is a new kinetoplastid-specific subunit of the single trypanosomal TIM complex that is involved in both the presequence as well as the mitochondrial carrier import pathway. TbTim15 is essential in the PCF and the BSF of trypanosomes. Our results are consistent with the idea that TbTim15 might be an IMS-localized protein import receptor. However, direct demonstration of the receptor function of TbTim15 and the identification of which substrates it recognizes require extensive biochemical analyses, which are beyond the scope of the present study.

4 | MATERIALS AND METHODS

4.1 | Transgenic cell lines

Transgenic *T. brucei* cell lines are based on the procyclic form (PCF) strain 29–13 (Wirtz et al., 1999) or the BSF strain F1γL262P (Dean et al., 2013). PCF cells were grown in SDM-79 (Schönenberger & Brun, 1979) at 27°C, BSF parasites were grown in HMI9 (Hirumi & Hirumi, 1989) at 37°C, both supplemented with 10% (v/v) fetal calf serum (FCS).

To produce plasmids for ectopic expression of C-terminal triple HA-tagged TbTim15 (Tb927.2.4445), putative TbTim20 (Tb927.11.1620), Tb927.8.7010, Tb927.11.1010, Tb927.11.16750, and Tb927.8.3450, the complete ORF of the respective gene was amplified by PCR. The PCR product was subsequently cloned into a modified pLew100 vector (Bochud-Allemann & Schneider, 2002; Wirtz et al., 1999), which contains a puromycin resistance gene and a triple HA-tag (Oberholzer et al., 2006). The triple HA-tagged LDH-DHFR fusion protein and the triple c-myc-tagged truncated (nt 274–912) ORF of MCP12 (Tb927.10.12840) have been described previously (Harsman et al., 2016). Cell lines expressing C-terminally myc-tagged TbPam27 and HA-tagged TbTim17 have been described before as well (Harsman et al., 2016; von Känel et al., 2020).

RNAi cell lines were generated using the same pLew100-derived vector described above and as described previously (von Känel et al., 2020; Wenger et al., 2023). The RNAi targets the indicated nt of the ORF of TbTim15 (nt 4–394), putative TbTim20 (nt 58–492), 7010 (nt 65–464) and 3450 (nt 22–412) or the 3′ untranslated region (UTR) of 1010 (nt +4–+292) and 16750 (nt +19–+260). The TbErv1 RNAi (Peikert et al., 2017), TbMic20 RNAi (Kaurov et al., 2018), and TbPam27 (von Känel et al., 2020) RNAi cell lines have been described previously.

4.2 | Antibodies

Polyclonal rabbit antiserum against TbPam27 and TbTim15 was commercially produced (Eurogentec, Belgium) using aa 128–142 (RFTTRQHKSRISYDE) and aa 119–133 (VGLIQRQRGRQEQRR) as antigens, respectively. For immunoblots (WB), the TbPam27

antiserum was used at a 1:200 and the TbTim15 antiserum at a 1:250–500 dilution. Commercially available antibodies were Mouse anti-c-myc (Invitrogen, dilution WB: 1:2000), mouse anti-HA (Sigma-Aldrich, dilution WB: 1:5000, dilution immunofluorescence (IF): 1:1000), and mouse anti-EF1a (Merck Millipore, dilution WB 1:10,000). Antibodies previously produced in our laboratory are polyclonal rabbit anti-ATOM40 (dilution WB: 1:10,000, dilution IF: 1:1000), polyclonal rabbit anti-ATOM69 (dilution WB: 1:50), polyclonal rabbit anti-VDAC (dilution WB: 1:1000), polyclonal rabbit anti-CoxIV (dilution WB: 1:1000), polyclonal rabbit anti-Cyt C (dilution WB 1:100), polyclonal rabbit anti-Tim9 (dilution WB: 1:40), polyclonal rabbit anti-TimRhom I (dilution WB: 1:150) and polyclonal rat anti-TbTim17 (dilution WB: 1:300) (Harsman et al., 2016; Mani et al., 2015; Niemann et al., 2013). Monoclonal anti-TbmHsp70 (dilution WB: 1:1000) (Panigrahi et al., 2008), polyclonal rabbit anti-MCP5 (dilution WB: 1:2500) (Peña-Diaz et al., 2012), polyclonal mouse anti-REAP1 (dilution WB: 1:1500) (Madison-Antenucci et al., 1998), polyclonal mouse anti-TbmHsp60 (Chanez et al., 2006), and polyclonal rabbit anti-LipDH (dilution WB: 1:5000) (Roldán et al., 2011) have been generated and described previously. Secondary antibodies used goat anti-mouse IRDye 680LT conjugated (LI-COR Biosciences, dilution WB: 1:20,000), goat anti-mouse Alexa Fluor 596 (ThermoFisher Scientific, dilution IF: 1000), goat anti-rabbit IRDye 800CW conjugated (LI-COR Biosciences, dilution WB 1:20,000), goat anti-rabbit Alexa Fluor 488 (Invitrogen, IF: 1:1000), and goat ani-rat IRDye 680LT conjugated (LI-COR biosciences, dilution WB 1:10,000). Immunoblots of BN-PAGE analysis were decorated with HRP-coupled goat anti-mouse or HRP-coupled goat anti-rabbit (both Sigma) as secondary antibodies (dilution: 1:5000).

4.3 | Digitonin, alkaline carbonate, and Triton X-100 extraction

Digitonin, alkaline carbonate, and Triton X-100 extractions have been done as described (Wenger et al., 2023).

4.4 | Co-immunoprecipitation (CoIP)

A mitochondria-enriched digitonin pellet from 1×10^8 cells expressing the protein of interest was solubilized in a buffer containing 20 mM Tris-HCl (pH 7.4), 0.1 mM EDTA, 100 mM NaCl, 10% glycerol, 1X Protease Inhibitor mix (Roche, EDTA-free), and 1% (w/v) digitonin for 15 min at 4°C. After centrifugation (20,000 g, 15 min, 4°C), the lysate was transferred to 50 µL HA bead slurry (anti-HA affinity matrix, Roche) or 30 µL c-myc bead slurry (EZview red anti-c-myc affinity gel, Sigma), which had been equilibrated in wash buffer (20 mM Tris–HCl (pH 7.4), 0.1 mM EDTA, 1 mM NaCl, 10% glycerol, 0.2% (w/v) digitonin). Subsequent to incubation in an end-over-end shaker for at least 1 h at 4°C, the supernatant containing the unbound proteins was removed. After washing the bead slurry three times with wash buffer, the bound proteins were eluted by boiling the resin for 5 min in 2% SDS in 60 mM Tris-HCl (pH6.8). 5% of both the input and the unbound proteins, and 100% of the IP sample were analyzed by SDS-PAGE and immunoblotting.

4.5 | Blue native (BN)-PAGE

BN-PAGE has been done as described (Harsman et al., 2016; Mani et al., 2015; von Känel et al., 2020; Wenger et al., 2023).

For analysis of the stalled presequence pathway intermediate, LDH-DHFR expression was induced by tetracycline and cell cultures were supplemented with 1 mM sulfanilamide and 50 µM aminopterine (AMT), 0.5 days before the experiment (Harsman et al., 2016; von Känel et al., 2020).

4.6 | Immunofluorescence (IF) microscopy

For analysis of the mitochondrial membrane potential, uninduced and induced TbTim15 RNAi cells were grown in the presence of 500 nM MitoTracker Red CMXRos. As a negative control, uninduced cells were treated with 40 µM carbonyl cyanide m-chlorophenylhydrazone (CCCP) before incubation with MitoTracker.

For antibody staining, cells were harvested, fixed with 4% paraformaldehyde in PBS and permeabilized with 0.2% Triton X-100 in PBS. Subsequently, the samples were decorated with primary antibodies for 1 h. Washing with PBS was followed by incubation with secondary antibody for 1 h. The cells were then post-fixed in cold methanol and mounted using VectaShield containing 4′,6-diamidino-2-phenylindole (DAPI) (Vector Laboratories). Images were acquired by a DMI6000B microscope and a DFC360 FX monochrome camera (both Leica Microsystems).

4.7 | RNA extraction and northern blotting

Acid guanidinium thiocyanate–phenol–chloroform extraction to isolate total RNA from uninduced and induced (2 days) RNAi cells was done as described elsewhere (Chomczynski & Sacchi, 1987). To determine RNAi efficiency, the resulting RNA was used for RT-PCR or northern blotting as described previously (Wenger et al., 2023).

4.8 | SILAC CoIP experiments

Cells inducibly expressing TbPam27-myc were washed in PBS and resuspended in SDM-80 (Lamour et al., 2005) supplemented with 5.55 mM glucose, 10% dialyzed FCS (BioConcept, Switzerland), and either light ($^{12}C_6/^{14}N_\chi$) or heavy ($^{13}C_6/^{15}N_\chi$) isotopes of arginine (1.1 mM) and lysine (0.4 mM) (Eurisotope). To make sure all proteins were completely labeled with heavy amino acids, the cells were grown in SILAC medium for 6–10 doubling times. TbPam27-myc expressing cells were induced for 1 day. About 4×10^8 uninduced and

4×10^8 induced cells were harvested and mixed. Subsequently, the mixture was extracted with Digitonin and subjected the co-IP protocol as describe above. The SILAC experiment was executed in three biological replicates including a label-switch and analyzed by liquid chromatography-mass spectrometry (LC–MS).

4.9 | LC–MS and data analysis

Eluates of TbPam27-myc CoIPs were subjected to SDS-PAGE, followed by staining of the proteins using colloidal Coomassie Blue. Gel lanes were cut into 10 equal slices followed by reduction, alkylation, and tryptic in-gel digestion of proteins as described (Peikert et al., 2017). LC–MS analyses were carried out using an UltiMate 3000 RSLCnano HPLC system (Thermo Scientific, Dreieich, Germany) connected to an Orbitrap Elite mass spectrometer (Thermo Scientific, Bremen, Germany). The RSLC system was operated with nanoEase M/Z Symmetry C18 precolumns (Waters, Eschborn, Germany; length of 20 mm, inner diameter of 180 µm, flow rate of 5–10 µL) for washing and preconcentration of peptides and a nanoEase M/Z HSS C18 T3 Col analytical column (Waters; length of 250 mm, inner diameter of 75 µm, particle size of 1.8 µm, packing density of 100 Å, flow rate of 300 nL/min) for peptide separation. Peptides were eluted using a binary solvent system consisting of 4% DMSO/0.1% formic acid (FA) (solvent A) and 48% methanol/30% acetonitrile/4% DMSO/0.1% FA (solvent B) and a gradient ranging from 1% to 65% B in 30 min, 65%–80% B in 5 min, and 3 min at 80% B. MS/MS data were obtained in data-dependent mode using the following parameters: full MS scans were acquired at a mass range of *m/z* 370–1700 at a resolution of 120,000 (at *m/z* 400), a maximum automatic gain control (AGC) of 1×10^6 ions, and a maximum injection time (IT) of 200 ms. A TOP15 method was applied for further fragmentation of multiply charged precursor ions by collision-induced dissociation. MS/MS scans were acquired with a normalized collision energy of 35%, an activation q of 0.25, an activation time of 10 ms, an AGC of 5000, and a maximum IT of 150 ms. The dynamic exclusion time was set to 45 s.

Mass spectrometric raw data were processed using MaxQuant/Andromeda (Cox et al., 2011; Cox & Mann, 2008, version 1.5.5.1) and searched against all entries in the TriTryp database (https://tritrypdb.org, version 8.1) for peptide and protein identification using MaxQuant default parameters and Arg10 and Lys8 as heavy labels. The options "re-quantify" and "match between runs" were enabled. Protein identification was based on ≥one unique peptide and a false discovery rate of 1% at peptide and protein level. SILAC-based relative protein quantification was based on unique peptides and ≥one ratio count (i.e., SILAC peptide pair). Proteins enriched in TbPam27-myc complexes were identified by applying the rank sum method (Breitling & Herzyk, 2005), carried out using the package 'RankProd' (version 3.24.0 Del Carratore et al., 2017) in R (version 4.2.2). *P* values and the percentage of false positives (i.e., *q*-values, referred to as adjusted *P* values) were determined for the enrichment of proteins quantified in at least two replicates. For a list of proteins identified and quantified, see Table S1.

AUTHOR CONTRIBUTIONS

André Schneider: Conceptualization; funding acquisition; writing – review and editing; supervision; visualization. **Corinne von Känel:** Conceptualization; investigation; writing – original draft; validation; writing – review and editing; supervision; methodology; visualization; formal analysis. **Silke Oeljeklaus:** Investigation; formal analysis; data curation; writing – review and editing; methodology. **Christoph Wenger:** Investigation; conceptualization; writing – review and editing. **Philip Stettler:** Conceptualization; investigation; visualization; writing – review and editing. **Anke Harsman:** Conceptualization; supervision; investigation; writing – review and editing. **Bettina Warscheid:** Writing – review and editing; supervision; funding acquisition; conceptualization.

ACKNOWLEDGEMENTS

We thank Julian Bender for assistance in bioinformatics data analysis. Work in the lab of A.S. was supported in part by NCCR RNA & Disease, a National Centre of Competence in Research (grant number 205601) and by project grant SNF 205200 both funded by the Swiss National Science Foundation. Open access funding provided by Universitat Bern.

CONFLICT OF INTEREST STATEMENT

The authors declare no conflict of interests.

DATA AVAILABILITY STATEMENT

The mass spectrometric data have been deposited to the ProteomeXchange Consortium (Deutsch et al., 2023; REF) via the PRIDE (Perez-Riverol et al., 2022) partner repository and are accessible using the dataset identifier PXD048257.

ETHICS STATEMENT

This is not a clinical study, no patients or animals were used in this study.

REFERENCES

Agarwala, R., Barrett T., Beck J., Benson D.A., Bollin C., Bolton E., et al. (2016) Database resources of the National Center for Biotechnology Information. *Nucleic Acids Research*, 44, D7–D19.

Allen, J.W.A., Ferguson, S.J. & Ginger, M.L. (2008) Distinctive biochemistry in the trypanosome mitochondrial intermembrane space suggests a model for stepwise evolution of the MIA pathway for import of cysteine-rich proteins. *FEBS Letters*, 582, 2817–2825.

Allen, S., Balabanidou, V., Sideris, D.P., Lisowsky, T. & Tokatlidis, K. (2005) Erv1 mediates the Mia40-dependent protein import pathway and provides a functional link to the respiratory chain by shuttling electrons to cytochrome c. *Journal of Molecular Biology*, 353, 937–944.

Banerjee, R., Gladkova, C., Mapa, K., Witte, G. & Mokranjac, D. (2015) Protein translocation channel of mitochondrial inner membrane and matrix-exposed import motor communicate via two-domain coupling protein. *eLife*, 4, e11897.

Basu, S., Leonard, J.C., Desai, N., Mavridou, D.A.I., Tang, K.H., Goddard, A.D. et al. (2013) Divergence of Erv1-associated mitochondrial import and export pathways in trypanosomes and anaerobic protists. *Eukaryotic Cell*, 12, 343–355.

Blum, M., Chang, H.Y., Chuguransky, S., Grego, T., Kandasaamy, S., Mitchell, A. et al. (2021) The InterPro protein families and domains database: 20 years on. *Nucleic Acids Research*, 49, 344–354.

Bochud-Allemann, N. & Schneider, A. (2002) Mitochondrial substrate level phosphorylation is essential for growth of procyclic *Trypanosoma brucei**. *Journal of Biological Chemistry*, 277, 32849–32854.

Breitling, R. & Herzyk, P. (2005) Rank-based methods as a non-parametric alternative of the T-statistic for the analysis of biological microarray data. *Journal of Bioinformatics and Computational Biology*, 3, 1171–1189.

Burki, F., Roger, A.J., Brown, M.W. & Simpson, A.G.B. (2020) The new tree of eukaryotes. *Trends in Ecology & Evolution*, 35, 43–55.

Ceh-Pavia, E., Tang, X., Liu, Y., Heyes, D.J., Zhao, B., Xiao, P. et al. (2020) Redox characterisation of Erv1, a key component for protein import and folding in yeast mitochondria. *The FEBS Journal*, 287, 2281–2291.

Chanez, A.L., Hehl, A.B., Engstler, M. & Schneider, A. (2006) Ablation of the single dynamin of *T. brucei* blocks mitochondrial fission and endocytosis and leads to a precise cytokinesis arrest. *Journal of Cell Science*, 119, 2968–2974.

Chomczynski, P. & Sacchi, N. (1987) Single-step method of RNA isolation by acid guanidinium thiocyanate-phenol-chloroform extraction. *Analytical Biochemistry*, 162, 156–159.

Claros, M.G. & Vincens, P. (1996) Computational method to predict mitochondrially imported proteins and their targeting sequences. *European Journal of Biochemistry*, 241, 779–786.

Cox, J. & Mann, M. (2008) MaxQuant enables high peptide identification rates, individualized p.p.b.-range mass accuracies and proteome-wide protein quantification. *Nature Biotechnology*, 26, 1367–1372.

Cox, J., Neuhauser, N., Michalski, A., Scheltema, R.A., Olsen, J.V. & Mann, M. (2011) Andromeda: a peptide search engine integrated into the MaxQuant environment. *Journal of Proteome Research*, 10, 1794–1805.

Craig, E.A. (2018) Hsp70 at the membrane: driving protein translocation. *BMC Biology*, 16, 1–11.

Cristodero, M., Seebeck, T. & Schneider, A. (2010) Mitochondrial translation is essential in bloodstream forms of *Trypanosoma brucei*. *Molecular Microbiology*, 78, 757–769.

Dean, S., Gould, M.K., Dewar, C.E. & Schnaufer, A.C. (2013) Single point mutations in ATP synthase compensate for mitochondrial genome loss in trypanosomes. *Proceedings of the National Academy of Sciences of the United States of America*, 110, 14741–14746.

Del Carratore, F., Jankevics, A., Eisinga, R., Heskes, T., Hong, F. & Breitling, R. (2017) RankProd 2.0: a refactored bioconductor package for detecting differentially expressed features in molecular profiling datasets. *Bioinformatics*, 33, 2774–2775.

Deutsch, E.W., Bandeira, N., Perez-Riverol, Y., Sharma, V., Carver, J.J., Mendoza, L. et al. (2023) The ProteomeXchange consortium at 10 years: 2023 update. *Nucleic Acids Research*, 51, D1539–D1548.

D'Silva, P.D., Schilke, B., Walter, W., Andrew, A. & Craig, E.A. (2003) J protein cochaperone of the mitochondrial inner membrane required for protein import into the mitochondrial matrix. *Proceedings of the National Academy of Sciences of the United States of America*, 100, 13839–13844.

Eaglesfield, R. & Tokatlidis, K. (2021) Targeting and insertion of membrane proteins in mitochondria. *Frontiers in Cell and Development Biology*, 9.

Emanuelsson, O., Brunak, S., von Heijne, G. & Nielsen, H. (2007) Locating proteins in the cell using TargetP, SignalP and related tools. *Nature Protocols*, 2, 953–971.

Fenn, K. & Matthews, K.R. (2007) The cell biology of *Trypanosoma brucei* differentiation. *Current Opinion in Microbiology*, 10, 539–546.

Ferramosca, A. & Zara, V. (2013) Biogenesis of mitochondrial carrier proteins: molecular mechanisms of import into mitochondria. *Biochimica et Biophysica Acta*, 1833, 494–502.

Frazier, A.E., Dudek, J., Guiard, B., Voos, W., Li, Y., Lind, M. et al. (2004) Pam16 has an essential role in the mitochondrial protein import motor. *Nature Structural & Molecular Biology*, 11, 226–233.

Fukasawa, Y., Oda, T., Tomii, K. & Imai, K. (2017) Origin and evolutionary alteration of the mitochondrial import system in eukaryotic lineages. *Molecular Biology and Evolution*, 34, 1574–1586.

Gabler, F., Nam, S.Z., Till, S., Mirdita, M., Steinegger, M., Söding, J. et al. (2020) Protein sequence analysis using the MPI bioinformatics toolkit. *Current Protocols in Bioinformatics*, 72, e108.

Gentle, I.E., Perry, A.J., Alcock, F.H., Likic, V.A., Dolezal, P., Ng, E.T. et al. (2007) Conserved motifs reveal details of ancestry and structure in the small TIM chaperones of the mitochondrial intermembrane space. *Molecular Biology and Evolution*, 24, 1149–1160.

Gupta, A. & Becker, T. (2021) Mechanisms and pathways of mitochondrial outer membrane protein biogenesis. *Biochimica et Biophysica Acta*, 1862, 148323.

Hansen, K.G. & Herrmann, J.M. (2019) Transport of proteins into mitochondria. *The Protein Journal*, 38, 330–342.

Harsman, A., Oeljeklaus, S., Wenger, C., Huot, J.L., Warscheid, B. & Schneider, A. (2016) The non-canonical mitochondrial inner membrane presequence translocase of trypanosomatids contains two essential rhomboid-like proteins. *Nature Communications*, 7, 1–13.

Harsman, A. & Schneider, A. (2017) Mitochondrial protein import in trypanosomes: expect the unexpected. *Traffic*, 18, 96–109.

Hirumi, H. & Hirumi, K. (1989) Continuous cultivation of *Trypanosoma brucei* blood stream forms in a medium containing a low concentration of serum protein without feeder cell layers. *Journal of Parasitology*, 75, 985–989.

Horst, M., Oppliger, W., Rospert, S., Schönfeld, H.J., Schatz, G. & Azem, A. (1997) Sequential action of two Hsp70 complexes during protein import into mitochondria. *The EMBO Journal*, 16, 1842–1849.

Kang, P.J., Ostermann, J., Shilling, J., Neupert, W., Craig, E.A. & Pfanner, N. (1990) Requirement for Hsp70 in the mitochondrial matrix for translocation and folding of precursor proteins. *Nature*, 348, 137–143.

Kaurov, I., Heller, J., Deisenhammer, S., Potěšil, D., Zdráhal, Z. & Hashimi, H. (2022) The essential cysteines in the CIPC motif of the thioredoxin-like *Trypanosoma brucei* MICOS subunit TbMic20 do not form an intramolecular disulfide bridge in vivo. *Molecular and Biochemical Parasitology*, 248, 111463.

Kaurov, I., Vancová, M., Schimanski, B., Cadena, L.R., Heller, J., Bílý, T. et al. (2018) The diverged trypanosome MICOS complex as a hub for mitochondrial cristae shaping and protein import. *Current Biology*, 28, 3393–3407.

Khalimonchuk, O. & Winge, D.R. (2008) Function and redox state of mitochondrial localized cysteine-rich proteins important in the assembly of cytochrome c oxidase. *Biochimica et Biophysica Acta*, 1783, 618–628.

Krogh, A., Larsson, B., von Heijne, G. & Sonnhammer, E.L.L. (2001) Predicting transmembrane protein topology with a hidden Markov model: application to complete genomes. *Journal of Molecular Biology*, 305, 567–580.

Laloraya, S., Dekker, P.J.T., Voos, W., Craig, E.A. & Pfanner, N. (1995) Mitochondrial GrpE modulates the function of matrix Hsp70 in translocation and maturation of preproteins. *Molecular and Cellular Biology*, 15, 7098–7105.

Laloraya, S., Gambill, B.D. & Craig, E.A. (1994) A role for a eukaryotic GrpE-related protein, Mge1p, in protein translocation. *Proceedings of the National Academy of Sciences of the United States of America*, 91, 6481–6485.

Lamour, N., Rivière, L., Coustou, V., Coombs, G.H., Barrett, M.P. & Bringaud, F. (2005) Proline metabolism in procyclic *Trypanosoma brucei* is down-regulated in the presence of glucose. *The Journal of Biological Chemistry*, 280, 11902–11910.

Letunic, I., Khedkar, S. & Bork, P. (2021) SMART: recent updates, new developments and status in 2020. *Nucleic Acids Research*, 49, 458–460.

Lithgow, T., Junne, T., Wachter, C. & Schatz, G. (1994) Yeast mitochondria lacking the two import receptors Mas20p and Mas70p can efficiently and specifically import precursor proteins. *Journal of Biological Chemistry*, 269, 15325–15330.

Longen, S., Bien, M., Bihlmaier, K., Kloeppel, C., Kauff, F., Hammermeister, M. et al. (2009) Systematic analysis of the twin Cx9C protein family. *Journal of Molecular Biology*, 393, 356–368.

Madison-Antenucci, S., Sabatini, R.S., Pollard, V.W. & Hajduk, S.L. (1998) Kinetoplastid RNA-editing-associated protein 1 (REAP-1): a novel editing complex protein with repetitive domains. *EMBO Journal*, 17, 6368–6376.

Mani, J., Desy, S., Niemann, M., Chanfon, A., Oeljeklaus, S., Pusnik, M. et al. (2015) Mitochondrial protein import receptors in Kinetoplastids reveal convergent evolution over large phylogenetic distances. *Nature Communications*, 6, 1–12.

Mani, J., Meisinger, C. & Schneider, A. (2016) Peeping at TOMs—diverse entry gates to mitochondria provide insights into the evolution of eukaryotes. *Molecular Biology and Evolution*, 33, 337–351.

Mani, J., Rout, S., Desy, S. & Schneider, A. (2017) Mitochondrial protein import - functional analysis of the highly diverged Tom22 orthologue of *Trypanosoma brucei*. *Scientific Reports*, 7, 1–12.

Marom, M., Azem, A. & Mokranjac, D. (2011) Understanding the molecular mechanism of protein translocation across the mitochondrial inner membrane: still a long way to go. *Biochimica et Biophysica Acta*, 1808, 990–1001.

Modjtahedi, N., Tokatlidis, K., Dessen, P. & Kroemer, G. (2016) Mitochondrial proteins containing coiled-coil-helix-coiled-coil-helix (CHCH) domains in health and disease. *Trends in Biochemical Sciences*, 41, 245–260.

Niemann, M., Wiese, S., Mani, J., Chanfon, A., Jackson, C., Meisinger, C. et al. (2013) Mitochondrial outer membrane proteome of *Trypanosoma brucei* reveals novel factors required to maintain mitochondrial morphology. *Molecular & Cellular Proteomics*, 12, 515–528.

Oberholzer, M., Morand, S., Kunz, S. & Seebeck, T. (2006) A vector series for rapid PCR-mediated C-terminal in situ tagging of *Trypanosoma brucei* genes. *Molecular and Biochemical Parasitology*, 145, 117–120.

Okamoto, H., Miyagawa, A., Shiota, T., Tamura, Y. & Endo, T. (2014) Intramolecular disulfide bond of Tim22 protein maintains integrity of the TIM22 complex in the mitochondrial inner membrane. *The Journal of Biological Chemistry*, 289, 4827–4838.

Panigrahi, A.K., Zíková, A., Dalley, R.A., Acestor, N., Ogata, Y., Anupama, A. et al. (2008) Mitochondrial complexes in *Trypanosoma brucei*: a novel complex and a unique oxidoreductase complex. *Molecular & Cellular Proteomics*, 7, 534–545.

Peikert, C.D., Mani, J., Morgenstern, M., Käser, S., Knapp, B., Wenger, C. et al. (2017) Charting organellar importomes by quantitative mass spectrometry. *Nature Communications*, 8, 15272.

Peleh, V., Cordat, E. & Herrmann, J.M. (2016) Mia40 is a trans-site receptor that drives protein import into the mitochondrial intermembrane space by hydrophobic substrate binding. *eLife*, 5.

Peleh, V., Zannini, F., Backes, S., Rouhier, N. & Herrmann, J.M. (2017) Erv1 of Arabidopsis thaliana can directly oxidize mitochondrial intermembrane space proteins in the absence of redox-active Mia40. *BMC Biology*, 15, 1–14.

Peña-Diaz, P., Pelosi, L., Ebikeme, C., Colasante, C., Gao, F., Bringaud, F. et al. (2012) Functional characterization of TbMCP5, a conserved and essential ADP/ATP carrier present in the mitochondrion of the human pathogen *Trypanosoma brucei*. *Journal of Biological Chemistry*, 287, 41861–41874.

Perez-Riverol, Y., Bai, J., Bandla, C., García-Seisdedos, D., Hewapathirana, S., Kamatchinathan, S. et al. (2022) The PRIDE database resources in 2022: a hub for mass spectrometry-based proteomics evidences. *Nucleic Acids Research*, 50, D543–D552.

Petrungaro, C., Zimmermann, K.M., Küttner, V., Fischer, M., Dengjel, J., Bogeski, I. et al. (2015) The Ca(2+)-dependent release of the Mia40-induced MICU1-MICU2 Dimer from MCU regulates mitochondrial Ca(2+) uptake. *Cell Metabolism*, 22, 721–733.

Pyrihová, E., Motyčková, A., Voleman, L., Wandyszewska, N., Fišer, R., Seydlová, G. et al. (2018) A single TIM translocase in the mitosomes of Giardia intestinalis illustrates convergence of protein import machines in anaerobic eukaryotes. *Genome Biology and Evolution*, 10, 2813–2822.

Roger, A.J., Muñoz-Gómez, S.A. & Kamikawa, R. (2017) The origin and diversification of mitochondria. *Current Biology*, 27, 1177–1192.

Roldán, A., Comini, M.A., Crispo, M. & Krauth-Siegel, R.L. (2011) Lipoamide dehydrogenase is essential for both bloodstream and procyclic *Trypanosoma brucei*. *Molecular Microbiology*, 81, 623–639.

Schnaufer, A., Domingo, G.J. & Stuart, K. (2002) Natural and induced dyskinetoplastic trypanosomatids: how to live without mitochondrial DNA. *International Journal for Parasitology*, 32, 1071–1084.

Schneider, A. (2018) Mitochondrial protein import in trypanosomatids: variations on a theme or fundamentally different? *PLoS Pathogens*, 14, e1007351.

Schneider, A. (2020) Evolution of mitochondrial protein import—lessons from trypanosomes. *Biological Chemistry*, 401, 663–676.

Schneider, H.C., Westermann, B., Neupert, W. & Brunner, M. (1996) The nucleotide exchange factor MGE exerts a key function in the ATP-dependent cycle of mt-Hsp70-Tim44 interaction driving mitochondrial protein import. *The EMBO Journal*, 15, 5796–5803.

Schönenberger, M. & Brun, R. (1979) Cultivation and in vitro cloning of procyclic culture forms of '*Trypanosoma brucei*' in a semi-defined medium: short communication. *Acta Tropica*, 36, 289–292.

Schulz, C., Schendzielorz, A. & Rehling, P. (2015) Unlocking the presequence import pathway. *Trends in Cell Biology*, 25, 265–275.

Shannon, P., Markiel, A., Ozier, O., Baliga, N.S., Wang, J.T., Ramage, D. et al. (2003) Cytoscape: a software environment for integrated models of biomolecular interaction networks. *Genome Research*, 13, 2498–2504.

Singha, U.K., Hamilton, V. & Chaudhuri, M. (2015) Tim62, a novel mitochondrial protein in *Trypanosoma brucei*, is essential for assembly and stability of the TbTim17 protein complex. *The Journal of Biological Chemistry*, 290, 23226–23239.

Singha, U.K., Hamilton, V.N., Duncan, M.R., Weems, E., Tripathi, M.K. & Chaudhuri, M. (2012) Protein translocase of mitochondrial inner membrane in *Trypanosoma brucei*. *The Journal of Biological Chemistry*, 287, 14480–14493.

Singha, U.K., Peprah, E., Williams, S., Walker, R., Saha, L. & Chaudhuri, M. (2008) Characterization of the mitochondrial inner membrane protein translocator Tim17 from *Trypanosoma brucei*. *Molecular and Biochemical Parasitology*, 159, 30–43.

Singha, U.K., Tripathi, A., Smith, J.T., Jr., Quinones, L., Saha, A., Singha, T. et al. (2021) Novel IM-associated protein Tim54 plays a role in the mitochondrial import of internal signal-containing proteins in *Trypanosoma brucei*. *Biology of the Cell*, 113, 39–57.

Smith, J.T., Singha, U.K., Misra, S. & Chaudhuri, M. (2018) Divergent small Tim homologues are associated with TbTim17 and critical for the biogenesis of TbTim17 protein complexes in *Trypanosoma brucei*. *mSphere*, 3.

Szklarczyk, R., Wanschers, B.F.J., Nabuurs, S.B., Nouws, J., Nijtmans, L.G. & Huynen, M.A. (2011) NDUFB7 and NDUFA8 are located at the intermembrane surface of complex I. *FEBS Letters*, 585, 737–743.

Truscott, K.N., Voos, W., Frazier, A.E., Lind, M., Li, Y., Geissler, A. et al. (2003) A J-protein is an essential subunit of the presequence translocase–associated protein import motor of mitochondria. *The Journal of Cell Biology*, 163, 707–713.

Turra, G.L., Liedgens, L., Sommer, F., Schneider, L., Zimmer, D., Vilurbina Perez, J. et al. (2021) In vivo structure–function analysis and redox interactomes of leishmania tarentolae Erv. *Microbiology Spectrum*, 9, e0080921.

van der Bliek, A.M., Sedensky, M.M. & Morgan, P.G. (2017) Cell biology of the mitochondrion. *Genetics*, 207, 843–871.

Vögtle, F.N., Wortelkamp, S., Zahedi, R.P., Becker, D., Leidhold, C., Gevaert, K. et al. (2009) Global analysis of the mitochondrial N-proteome identifies a processing peptidase critical for protein stability. *Cell*, 139, 428–439.

von Känel, C., Muñoz-Gómez, S.A., Oeljeklaus, S., Wenger, C., Warscheid, B., Wideman, J.G. et al. (2020) Homologue replacement in the import motor of the mitochondrial inner membrane of trypanosomes. *eLife*, 9.

Wenger, C., Harsman, A., Niemann, M., Oeljeklaus, S., von Känel, C., Calderaro, S. et al. (2023) The Mba1 homologue of *Trypanosoma brucei* is involved in the biogenesis of oxidative phosphorylation complexes. *Molecular Microbiology*, 119, 537–550.

Wenger, C., Oeljeklaus, S., Warscheid, B., Schneider, A. & Harsman, A. (2017) A trypanosomal orthologue of an intermembrane space chaperone has a non-canonical function in biogenesis of the single mitochondrial inner membrane protein translocase. *PLoS Pathogens*, 13, e1006550.

Wheeler, R.J. (2021) A resource for improved predictions of Trypanosoma and Leishmania protein three-dimensional structure. *PLoS One*, 16, e0259871.

Wiedemann, N. & Pfanner, N. (2017) Mitochondrial machineries for protein import and assembly. *Annual Review of Microbiology*, 86, 685–714.

Wirtz, E., Leal, S., Ochatt, C. & Cross, G.A.M. (1999) A tightly regulated inducible expression system for conditional gene knock-outs and dominant-negative genetics in *Trypanosoma brucei*. *Molecular and Biochemical Parasitology*, 99, 89–101.

Wrobel, L., Trojanowska, A., Sztolsztener, M.E. & Chacinska, A. (2013) Mitochondrial protein import: Mia40 facilitates Tim22 translocation into the inner membrane of mitochondria. *Molecular Biology of the Cell*, 24, 543–554.

Žárský, V. & Doležal, P. (2016) Evolution of the Tim17 protein family. *Biology Direct*, 11, 54.

Zimmermann, R. & Neupert, W. (1980) Transport of proteins into mitochondria: posttranslational transfer of ADP/ATP carrier into mitochondria in vitro. *European Journal of Biochemistry*, 109, 217–229.

SUPPORTING INFORMATION

Additional supporting information can be found online in the Supporting Information section at the end of this article.

How to cite this article: von Känel, C., Oeljeklaus, S., Wenger, C., Stettler, P., Harsman, A., Warscheid, B. et al. (2024) Intermembrane space-localized TbTim15 is an essential subunit of the single mitochondrial inner membrane protein translocase of trypanosomes. *Molecular Microbiology*, 00, 1–15. Available from: https://doi.org/10.1111/mmi.15262